The FORCAST mid-infrared facility instrument and in-flight performance on SOFIA

Joseph D. Adams[a], Terry L. Herter[a], George E. Gull[a], Justin Schoenwald[a], Charles P. Henderson[a], Luke D. Keller[b], James M. De Buizer[c], Gordon J. Stacey[a], Thomas Nikola[a], William Vacca[c], L. Hirsch[a], J. Wang[a], L. Andrew Helton[c]

[a]Department of Astronomy, Cornell University,
105 Space Sciences Building, Ithaca, NY, USA 14853-6801

[b]Department of Physics, Ithaca College, 264 Center for Natural Sciences, Ithaca, NY, USA 14850

[c]Universities Space Research Association, NASA Ames Research Center,
Building N232, Moffett Field, CA, USA 94035-0001

ABSTRACT

FORCAST has completed 16 engineering and science flights as the "First Light" U. S. science instrument aboard SOFIA and will be commissioned as a SOFIA facility instrument in 2013. FORCAST offers dual channel imaging (diffraction-limited at wavelengths > 15 microns) using a 256 x 256 pixel Si:As blocked impurity band (BIB) detector at 5 - 28 microns and a 256 x 256 pixel Si:Sb BIB detector at 28 - 40 microns. FORCAST images a 3.4 arcmin × 3.2 arcmin field-of-view on SOFIA with a rectified plate scale of 0.768 arcsec/pixel. In addition to imaging capability, FORCAST offers a facility mode for grism spectroscopy that will commence during SOFIA Cycle 1. The grism suite enables spectroscopy over nearly the entire FORCAST wavelength range at low resolution (~140 - 300). Optional cross-dispersers boost the spectroscopic resolution to ~1200 at 5 - 8 microns and ~800 at 9.8 – 13.7 microns. Here we describe the FORCAST instrument including observing modes for SOFIA Cycle 1. We also summarize in-flight results, including detector and optical performance, sensitivity performance, and calibration.

Keywords: Infrared cameras, blocked impurity band detectors, metal mesh filters

1. INTRODUCTION

The **F**aint **O**bject infra**R**ed **CA**mera for the **S**ofia **T**elescope (FORCAST) is a dual-channel, wide-field camera designed to perform imaging in the infrared from 5 - 40 μm. FORCAST will be a facility instrument on the **S**tratospheric **O**bservatory **F**or **I**nfrared **A**stronomy (SOFIA). Our focus in this paper is to describe FORCAST as a facility instrument and report in-flight performance results to date. We begin with a very brief description of FORCAST; for a more detailed description of the instrument design, see Keller *et al.* (2002)[1], Keller *et al.* (2004)[2], and Adams *et al.* (2006)[3].

FORCAST is a cryogenic (4 K work surface and 77 K radiation shield), two-channel camera and grism spectrometer. The two channels have identical optical prescriptions. We use two detector arrays, a Si:As blocked impurity band (BIB) array for $\lambda < 28$ μm and a Si:Sb BIB array for $\lambda \geq 28$ μm. Herter *et al*. (1998)[4] present a review of BIB detectors for astronomy. Each array has a format of 256 × 256 pixels. Due to anamorphic magnification, the field-of-view is 3.4′ × 3.2′; the rectified plate scale is 0.768″/pixel after image processing. Simultaneous imaging in two bands (5-28 μm and 28-40 μm) is enabled using a cold (4 K) dichroic beamsplitter to split the telescope beam to the long wavelength channel (LWC) and the short wavelength channel (SWC). Our design enables high efficiency observations and takes advantage of the increased performance, relative to Si:Sb, of the Si:As BIB array for $\lambda < 28$ μm. Table 1 summarizes the FORCAST operational parameters. Single channel imaging for higher throughput is possible by sliding the dichroic out of the beam and inserting a mirror (SWC) or an open aperture (LWC). This operation can be performed on-the-fly. FORCAST allows selection of the wavelength bandpass independently for each channel via cryogenic filter wheels. Up to 10 filters and grisms can be installed in each channel. The available filter bandpasses cover several PAH features as well as continuum features.

Table 1. Overview of FORCAST characteristics.

Specification	SWC	LWC	Units
Detector Type	Si:As	Si:Sb	
Wavelength Range	5 - 28	28 - 40	μm
Well Size (Low Capacitance)	1.9×10^6	1.9×10^6	e-
Well Size (High Capacitance)	1.8×10^7	1.8×10^7	e-
Pixel width (square pixels)	50	50	μm
Plate scale (rectified)	0.768	0.768	arcsec/pixel
Array Size	256 × 256	256 × 256	pixels
Mulitplexer Readout	16	16	Channels
Field of View/Array	3.4 × 3.2	3.4 × 3.2	arcmin

FORCAST is equipped with a pupil viewer in each channel consisting of a lens that images the Lyot stop onto the detector. The pupil viewers were used to align the FORCAST collimator mirror with the secondary mirror of the telescope. Additionally, the pupil viewers are used to measure the emissivity of the telescope by providing the ability to measure telescope and sky emission independently.

We have developed a sensitivity model to calculate the expected in-flight point source sensitivity of FORCAST. The model includes the transmission and thermal emission of the atmosphere; telescope emission and image quality; and the measured (when possible) or expected performance of the optics and detectors. Atmospheric transmission was determined using ATRAN software (Lord 1992)[5]. We measured the filter transmission curves at room temperature using a Fourier Transform Spectrometer. We have measured the dichroic transmission curve at 28 – 40 μm (room temperature) and reflection at 5 – 12 μm (T = 4 K). We use a scalar value of 0.86 for the dichroic reflection at 18 – 28 μm as measured in the laboratory. Quantum efficiency curves of Process Evaluation Chips were measured by the detector vendor (DRS Technologies, Anaheim, CA) and scaled to the quantum efficiency measured at Cornell for a bandpass filter (Adams *et al*. 2004)[6]. Table 2 shows the typical assumptions and performance values used to compute the point source sensitivity, while Table 3 lists the minimum detectable continuum flux (MDCF) necessary to achieve a signal-to-noise ratio of 4 in 900 seconds of integration time for each filter/dichroic configuration.

Table 2. Typical parameters used for the point source sensitivity model.

Parameter	Value
Source temperature	300 K
Altitude	41,000 ft.
Sky temperature	240 K
Water vapor overburden	7.1 μm
Primary mirror diameter	2.5 m
Elevation angle	40°
Telescope temperature	240 K
Telescope emissivity (estimated)	15%
Image quality (80% encircled energy)	5.3″
Window transmission	88%
Window temperature (estimated)	293 K
Window emissivity	6%
Reflectivity of each FORCAST internal mirror (all wavelengths)	97%
Read noise[6]	2400 e- (high capacitance) 245 e- (low capacitance)
Pixel size	50 μm
Excess noise βG^4	2.5

Table 3. Minimum Detectable Continuum Flux (MDCF) for the model parameters given in Table 2, corresponding to a signal-to-noise ratio of 4 in 900 seconds of integration time. The bandwidths were computed from our measured filter transmission curves, dichroic transmission curves, and detector quantum efficiencies; the effects of the spectral nature of the source and the atmosphere are excluded. These values are consistent with estimating the filter widths using their half-amplitude points (Herter et al. 2012)[7].

Filter Name (μm)	Bandwidth (μm)	Calculated MDCF (mJy)
Single Channel		
5.4	0.16	34.1
6.4	0.14	70.6
6.6	0.24	76.9
7.7	0.47	66.1
8.6	0.21	82.6
11.1	0.95	66.0
11.3	0.24	145
19.7	5.5	64.7
24.2	2.9	132
25.2	1.8	142
31.4	5.7	152
33.5	1.9	296
34.8	3.8	203
37.1	3.3	246
Dual Channel		
5.4	0.16	39.2
6.3	0.12	81.9
6.6	0.22	121
7.7	0.46	73.1
8.6	0.21	88.5
11.1	0.83	69.9
11.3	0.20	181
19.7	5.5	66.5
24.2	2.9	136
25.2	1.8	147
31.4	5.7	211
33.5	1.9	460
34.8	3.5	293
37.1	3.7	422

A suite of grisms for FORCAST has been developed to enable slit spectroscopy, which is now included as a facility mode. The grisms will be commissioned in 2013, at approximately the same time FORCAST imaging mode is commissioned. Grisms can be installed in the filter wheels with no modifications to the optics, but when installed, they each displace a broadband filter. Selection of filter/grism combinations for flight is driven by the science requirements for each cycle. The grisms cover most of the wavelengths accessible with FORCAST, at low to moderate resolution (Table 4). For details regarding the design, fabrication, and lab testing of the FORCAST grisms, see Ennico *et al.* (2006)[8], Ennico *et al.* (2007)[9], and Deen *et al.* (2008)[10]. Several slit masks are housed in the cryogenic wheel located at the field stop; the desired slit mask can be inserted into the beam on-the-fly. We have computed the MDCFs and minimum detectable line fluxes (MDLFs) for three wavelengths in each grism configuration. These performance values are listed in Table 5.

Table 4. Grism spectroscopic modes. The wavelength range for each mode is listed. For non-cross-dispersed modes, two slit sizes are available. The spectral resolution for each slit size is also listed.

Grism Mode	Wavelength Range (μm)	Slit	Spectral Resolution
G1	4.7 – 5.8	2.4″ × 192″	180
		4.7″ × 192″	90
G1xG2	4.7 – 5.8	2.4″ × 11.25″	1200
G3	8.4 – 13.7	2.4″ × 192″	300
		4.7″ × 192″	150
G3xG4	8.4 – 13.7	2.4″ × 11.25″	800
G5	17.6 – 27.7	2.4″ × 192″	140
		4.7″ × 192″	70
G6	28.7 – 37.1	2.4″ × 192″	220
		4.7″ × 192″	110

Table 5. Point source sensitivity estimates (S/N = 4 in 900 seconds of integration) calculated at three wavelengths spanning each grism spectroscopy mode for the two slit choices. The assumptions and inputs for these estimates are consistent with those in Table 2.

Grism Mode	λ (μm)	2.4″ Slit		4.7″ Slit	
		MDCF (mJy)	MDLF (10^{-16} W/m^2)	MDCF (mJy)	MDLF (10^{-16} W/m^2)
G1	5.1	98	2.9	79	2.3
G1	6.4	268	6.3	219	5.2
G1	7.7	724	6.3	496	5.2
G1xG2	5.1	238	1.2	-	-
G1xG2	6.4	703	2.8	-	-
G1xG2	7.7	918	3.0	-	-
G3	8.6	532	6.2	419	4.9
G3	11.0	575	5.2	449	4.1
G4	13.2	764	5.8	593	4.5
G3xG4	8.6	870	3.8	-	-
G3xG4	11.0	938	3.2	-	-
G3xG4	13.2	1239	3.5	-	-
G5	17.8	936	11	715	8.6
G5	22.8	989	9.3	834	7.9
G5	27.2	2586	20	1979	16
G6	28.9	1899	9.0	1365	6.5
G6	34.1	1994	8.0	1408	5.6
G6	37.0	2439	8.0	1763	5.6

2. OBSERVING MODES

For science observations, FORCAST requires chopping of the secondary mirror in order to move the target in the field-of-view, thereby allowing removal of the temporally-varying thermal background of the sky. Additionally, FORCAST requires a telescope nod in order to measure and remove spatial variations in thermal emission from the primary mirror caused by the motion of the chopping secondary mirror. For the general community, FORCAST operates in one of two observing modes. These modes are two-position chop and nod (C2N) and two-position chop, nod-off, two-position chop (C2NC2). C2N mode is commonly used for point sources and compact sources where the chop and nod throws are small enough (< 3.2′) so that all beams are contained in the field-of-view. Any chop and nod angle can be commanded in C2N mode, however the nod angle is frequently perpendicular to the chop angle (NPC) and rotated on the FORCAST focal

plane so that vertically-orientated detector artifacts (see §3.2) from a particular beam do not interfere with another beam. It is possible for the nod throw to match the chop throw (NMC) which superimposes 2 beams in the nod cycle, thereby increasing the signal-to-noise seen in the matched beams with respect to a single beam. C2NC2 mode is used for large sources when off-chip chop and nod throws are required. This mode utilizes the same sky sample for temporally adjacent on-source acquisitions, thereby increasing the duty time spent integrating on-source (~30%) with respect to the on-source duty time (25%) that would be spent integrating in C2N mode with off-chip chopping and nodding.

3. IN-FLIGHT PERFORMANCE

The SOFIA Early Science phase included science flights flown by the FORCAST and GREAT (Heyminck *et al*. 2012)[11] instruments. The FORCAST-allocated flights included 3 flights for science projects lead by the FORCAST team and a limited number of external collaborators ("Short Science"), and 10 flights dedicated to several guest investigators who were competitively awarded time through an allocation committee ("Basic Science"). For more details on SOFIA Early Science, see Young *et al*. (2012)[12].

3.1 Point Source Sensitivity

We have measured the signal-to-noise for all calibrators that were observed at altitudes greater than 41,000 ft during the 13 Early Science flights. The flux densities for the calibrators at each FORCAST wavelength were determined by integrating their measured spectra over the atmospheric transmission curve multiplied by the FORCAST system response. This enables us to estimate the minimum detectable continuum flux (MDCF) that can be observed at a given signal-to-noise ratio and integration time. Figure 1 shows the MDCF for each filter including the effects of using the dichroic on point source sensitivity. For comparison, we show the MDCFs predicted by the model described in §1. In general, the model predictions are realistic.

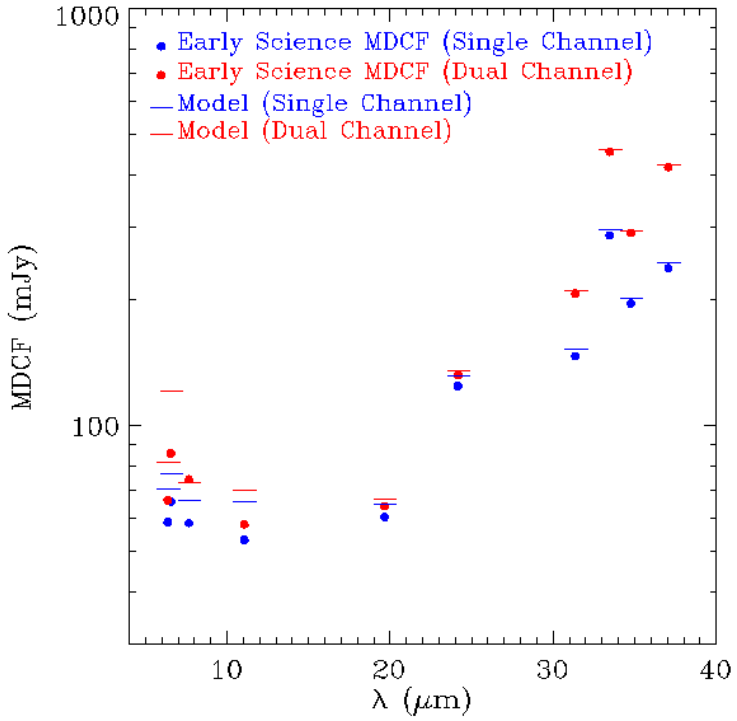

Figure 1. FORCAST in-flight point source sensitivity. The average minimum detectable continuum flux (MDCF) corresponding to a signal-to-noise ratio of 4 in 900 s integration time is shown for calibrator sources observed during Early Science at altitudes greater than 41,000 ft. Overlayed are the sensitivity model predictions for a typical case (Table 2).

3.2 Detector Performance

The gain dispersion β in BIB detectors can result in excess noise with respect to that of a standard Poisson noise distribution. The detective quantum efficiency is effectively η/β where η is the responsive quantum efficiency (Herter et al. 1998)[4]. The value of β depends on detector bias, well depth, and incident photon rate, whereby a higher number of incident photons on the detector generally results in a relatively higher β. Figure 2 shows the values of βG (where G is the detector gain) measured during Basic Science as a function of filter wavelength. Filter wavelength dependence is caused by variations in filter width, thermal background, and presence of the dichroic. In the laboratory (293 K flood illumination), typical values of βG are ~ 2.5. Lower values of βG are seen in flight due to the lower background caused by the colder temperatures of the sky and telescope and the lower emissivity of the atmosphere at altitude. Note that some measured values of βG are ≥ ~ 3 in-flight; these measurements are usually spurious due to optically variable background structure (see Figure 3). However, some of the brightest sources that were observed during Early Science (i.e. Jupiter) can also cause an increase in βG.

Several image artifacts were observed during Early Science (Figure 3). Multiplexer "droop" is the suppression of signal near the edges of a bright source caused by the presence of the source itself. Under high contrast conditions, as with a bright star or a bad pixel, multiplexer crosstalk is seen. This is a residual signal at the multiplexer output which decays in time. Both droop and crosstalk are corrected during pipeline processing. The crosstalk correction is performed using a channel median subtraction algorithm. In the case of an extended source, the source is first removed using a median filter

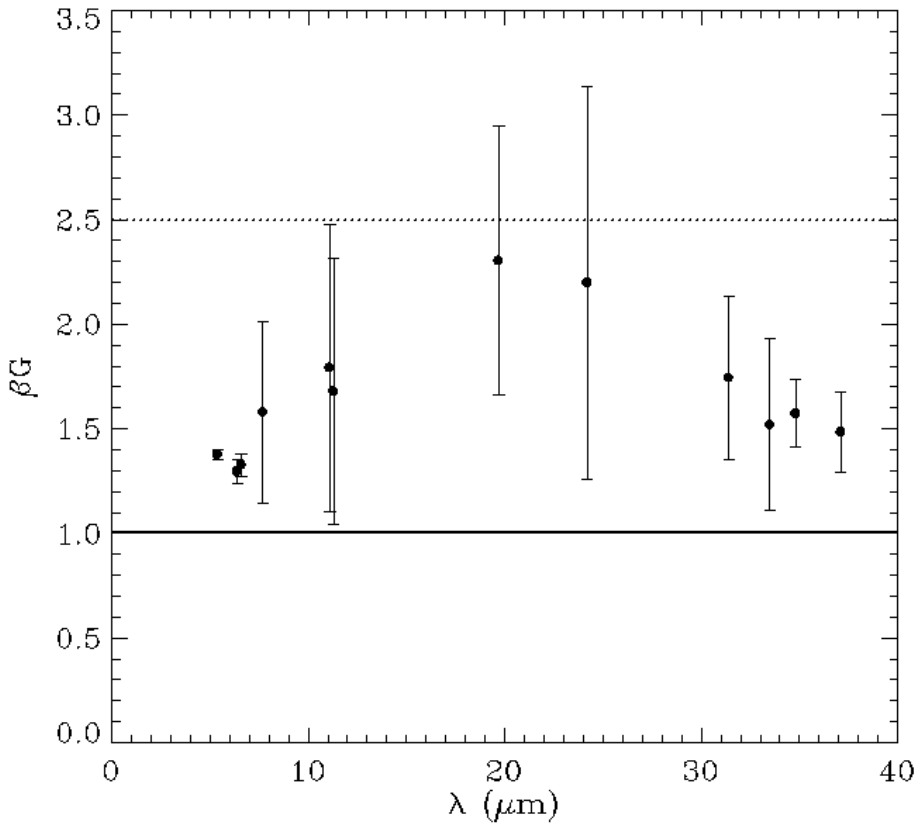

Figure 2. βG vs. filter in the calibrator images that were taken the 10 Basic Science flights. The solid line represents the performance of a true photovoltaic detector, while the dotted line represents the value that is assumed for the sensitivity model, which is based on laboratory measurements. Values of βG ≥ ~ 3 are usually spurious due to optically variable background structure (see Figure 3).

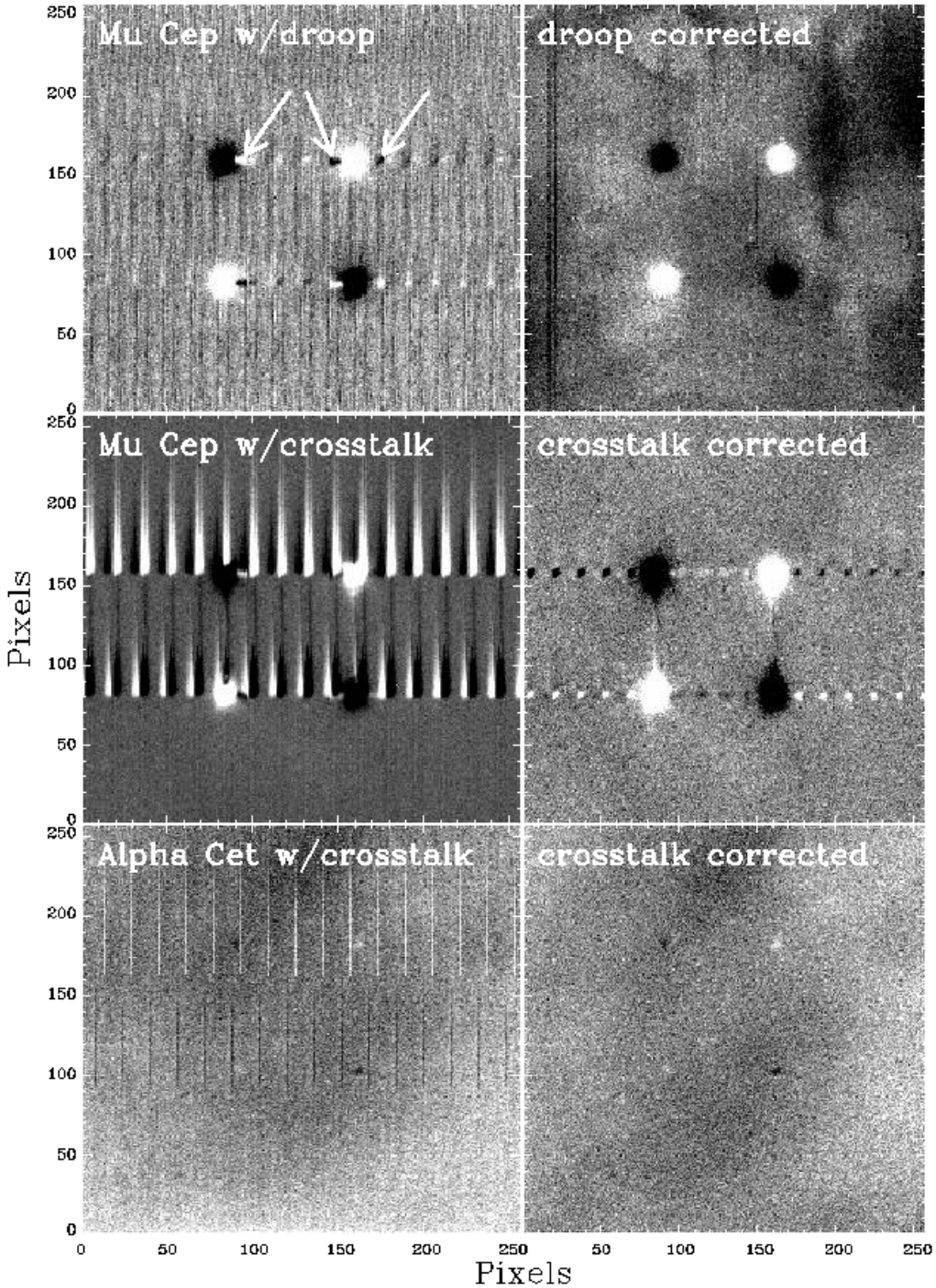

Figure 3. FORCAST (chop and nod subtracted) images showing detector artifacts. Top row: μ Cep at 11.1 μm showing image with droop (left) and with droop corrected (right). Middle row: μ Cep at 11.1 μm showing an image with multiplexer crosstalk associated with a bright point source (left) and with crosstalk removed (right). Bottom row: α Cet at 31.4 μm showing an image with multiplexer crosstalk from bad (dark) pixels (left) and with crosstalk removed (right). These images also show the background structure which is present in chop/nod differences due to variations in the thermal background at the pupil (see text).

subtraction across the frame and then re-added to the channel-subtracted image. These effects can also be mitigated by dithering and observing through a range of field angles at the focal plane. Finally, spatial variations in the background of integrated chop/nod differenced images were identified as temporal variations in the thermal signature near the edge of the pupil and in the secondary mirror struts (Figure 3 and Figure 4). We postulate the edge variations originate with tertiary mirror jitter. These variations can be removed for point sources using a box median filter subtraction; however, they impose a limit to detecting faint, extended sources such as debris disks. A hardware solution is required: during commissioning, we will install a new, undersized Lyot stop with strut masks that will block the thermal variations at the edge of the pupil and which will result in spatially flat chop/nod differences. Unfortunately, this will also reduce total optical throughput (by ~10%).

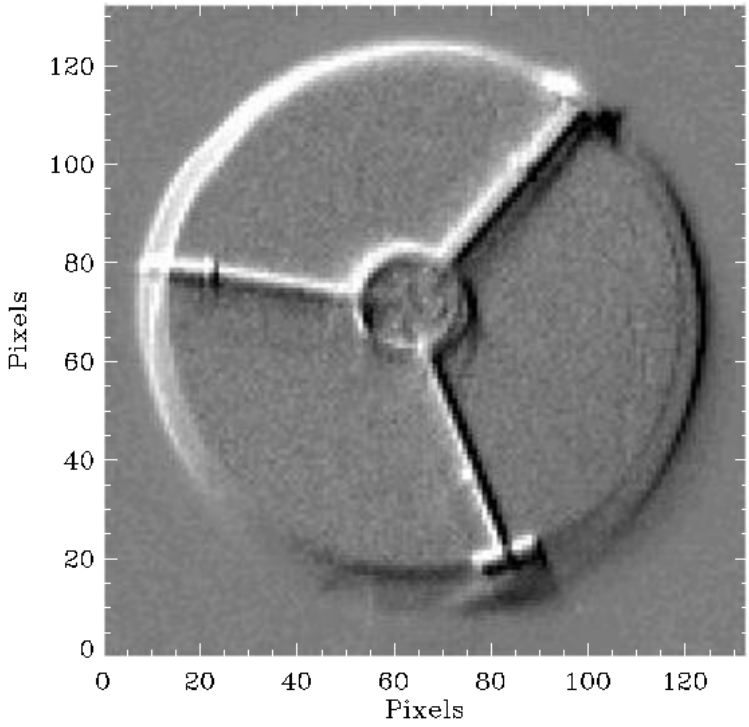

Figure 4. Temporally differenced pupil image at 11.3 μm taken during Basic Science Flight 60. Variations in thermal background due to motion at the edge of the pupil and movement of the secondary struts are seen as light and dark regions.

3.3 Distortion Correction

Both cameras in FORCAST contain off-axis, reflective optics (Keller *et al*. 2002)[1]. As a result, there is anamorphic magnification (6%) and nonlinear distortion (~ 1%) across the field-of-view. FORCAST contains a square pinhole grid test mask located at the field stop for the purposes of characterizing this field distortion. Using a polynomial warp fit to the image locations of the pinholes, we apply a distortion correction to the images during pipeline processing (Figure 5). This algorithm has achieved excellent results. After pipeline processing images of the pinhole mask, no systematic residuals were found in the rectification of the pinhole grid. The RMS pinhole spacing is square to 0.07 pixels (SWC) and 0.19 pixels in the LWC, including machining tolerances for the mask fabrication.

A check of the performance of the optical undistort algorithm was done on the sky using OMC-2, a star forming region north of the Orion Nebula containing several point sources (Adams *et al*. 2012)[13]. Using Spitzer/IRAC images to determine the “true” positions of these point sources, we applied tangent plane projection astrometric solutions to the pipeline-processed FORCAST images. The average position residual is 0.384″ for 19.7 μm and 0.379″ for 37.1 μm, indicating excellent rectification. The rectified plate scale is 0.768″/pixel.

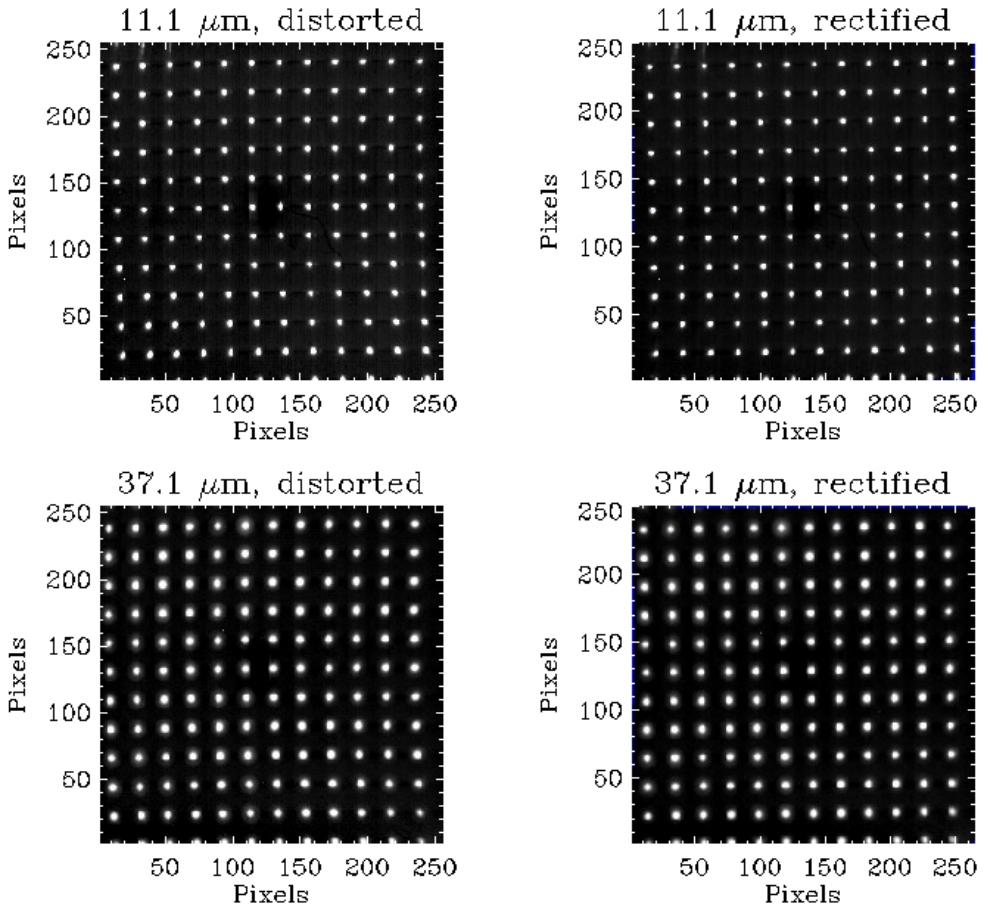

Figure 5. Distortion correction. Top row shows background-subtracted image of the pinhole grid at 11.1 μm (room temperature source) distorted (left) and rectified by the data reduction pipeline (right). Bottom rows shows the same for 37.1 μm, distorted (left) and rectified (right).

3.4 Calibration

FORCAST observes calibrator stars for flux calibration on several legs of each flight. The flux densities of the calibrator stars in each FORCAST filter were computed from model spectra of the stars and the measured instrument throughput. We performed photometry on all calibration stars that were observed during Early Science in order to derive the FORCAST calibration response. This calibration response is adjusted to that of a flat spectrum source (νF_ν = constant). Table 6 lists the average calibration response for each FORCAST filter that was used during Short Science. The RMS uncertainty in the calibration response values is ~ 7%, caused by variations in altitude, elevation angle, and water vapor burden. For Basic Science data, calibration was performed on a leg-by-leg basis and included corrections for altitude and elevation angle.

Using ATRAN models, (room temperature) filter transmission curves, and detector quantum efficiency curves (Adams *et al*. 2004)[6], we computed color corrections for objects that do not exhibit a flat spectrum across each bandpass. Note a paper dedicated to the topics of calibration and color corrections is in preparation (Vacca et al., in prep.). We discovered that the metal mesh filters (Adams *et al*. 2010)[14] have significant leaks at $\lambda < 5$ μm which require large color corrections for blue sources. We are therefore taking steps to mitigate these leaks, which include implementing a diamond dust scatter filter for the 24.2 μm mesh filter and using the order blocking filter normally used for Grism 5 with the 33.5, 34.8, and 37.1 μm mesh filters. The dichroic can also be used to block these leaks in the 33.5, 34.8, and 37.1 μm mesh filters. Finally, the 25.2 μm interference filter (procured from the U. Reading Multilayer Laboratory[15]) may be used in lieu of the 24.2 μm metal mesh filter.

Table 6. FORCAST calibration response used for Short Science, adjusted to a flat spectrum source (νF_ν = constant). 1 σ uncertainties are ± 7%. The 5.4 μm filter was not used with the dichroic during Short Science.

Filter	Response (single channel) (e-/s/mJy)	Response (dual channel) (e-/s/mJy)
5.4	310	-
6.4	245	192
6.6	265	142
7.7	484	380
11.1	643	568
11.3	163	125
19.7	1269	1110
24.2	599	481
31.4	505	235
33.5	81.0	32.5
34.8	230	111
37.1	112	48.0

ACKNOWLEDGMENTS

We thank the SOFIA telescope operators and mission operations team for their excellent work. This work is based on observations made with the NASA/DLR Stratospheric Observatory for Infrared Astronomy (SOFIA). SOFIA science mission operations are conducted jointly by the Universities Space Research Association (USRA), Inc., under NASA contract NAS2-97001, and the Deutsches SOFIA Institut (DSI) under DLR contract 50 OK 0901. Financial support for FORCAST was provided to Cornell University by NASA through award 8500-98-014 issued by USRA.

REFERENCES

[1] Keller, L. D., Herter, T. L., Stacey, G. J., Gull, G. E., Pirger, B., Schoenwald, J. and Nikola, T., "FORCAST: A Facility 5-40 micron camera for SOFIA," Proc. SPIE 4014, 86 (2002).

[2] Keller, L. D., Herter, T., Stacey, G., Gull, G., Schoenwald, J., Pirger, B., Adams, J., Berthoud, M., and Nikola, T., "First test results from FORCAST: the facility mid-IR camera for SOFIA," Proc. SPIE 5492, 1086 (2004).

[3] Adams, J. D., Herter, T. L., Keller, L. D., Gull, G. E., Pirger, B., Schoenwald, J., Berthoud, M., Stacy, G. J., and Nikola, T., "FORCAST: the facility mid-IR camera for SOFIA," Proc. SPIE 6269, 34 (2006).

[4] Herter, T. L., Hayward, T. L., Houck, J. R., Seib, D. H., and Lin, W. N., "Mid and far-infrared focal plane arrays for Astronomy," Proc. SPIE 3354, 109 (1998).

[5] Lord, S. D., NASA Technical Memorandum 103957 (1992).

[6] Adams, J. D., Herter, T. L., Keller, L. D., Gull, G. E., Pirger, B., Schoenwald, J., and Berthoud, M., "Testing of mid-infrared detector arrays for FORCAST," Proc. SPIE 5499, 442 (2004).

[7] Herter, T. L., Adams, J. D., De Buizer, J. M., Gull, G. E., Schoenwald, J., Henderson, C. P., Keller, L. D., Nikola, T., Stacey, G., and Vacca, W. D., "First Science Observations with SOFIA/FORCAST: The FORCAST Mid-infrared Camera," ApJ, 749L, 18 (2012)

[8] Ennico, K. A., Keller, L. D., Mar, D. J., Herter, T. L., Jaffe, D. T., Adams, J. D., and Greene, T. P., "Grism performance for mid-IR (5 - 40 micron) spectroscopy," Proc. SPIE 6269, 57 (2006).

[9] Ennico, K., Keller, L., Adams, J., Herter, T., Deen, C., Mar, D., Chitrakar, N., Jaffe, D., and Greene, T., "Grisms For FORCAST - A New Medium Resolution 5-40 Micron Spectroscopic Mode On SOFIA - Performance Testing," BAAS, 211, 1114 (2007).

[10] Deen, C. P., Jaffe, D. T., Marsh, J. P., Mar, D. J., Ennico, K. A., Greene, T. P., Keller, L., Chitrakar, N., Adams, J. D., and Herter, T., "A Silicon and KRS-5 Grism Suite for FORCAST on SOFIA," Proc. SPIE 7014, 81 (2008).

[11] Heyminck, S., Graf, U. U., Güsten, R., Stutzki, J., Hübers, H. W., and Hartogh, P., "GREAT: the SOFIA high-frequency heterodyne instrument," A&A, 542L, 1 (2012)

[12] Young, E., Becklin, E. E., Marcum, P. *et al*., "Early Science with SOFIA, the Stratospheric Observatory For Infrared Astronomy," ApJ, 749L, 17 (2012).
[13] Adams, J. D., Herter, T. L., Osorio, M. *et al*., "First Science Observations with SOFIA/FORCAST: Properties of Intermediate-luminosity Protostars and Circumstellar Disks in OMC-2," ApJ, 749L, 24 (2012)
[14] Adams, J. D., Herter, T. L., Gull, G. E., Schoenwald, J., Henderson, C. P., Keller, L. D., De Buizer, J. M., Stacey, G. J., & Nikola, T., "FORCAST: a first light instrument for SOFIA," Proc. SPIE 7735, 62 (2010)
[15] http://www.reading.ac.uk/infrared